DEVELOPMENTAL DYNAMICS 00:00–00, 2018
DOI: 10.1002/DVDY.24626

RESEARCH ARTICLE

ETV5 Regulates Ductal Morphogenesis With Sox9 and is Critical for Regeneration From Pancreatitis

Koushik K. Das,[1,2,3,4†] Steffen Heeg,[1,2,3,5†] Jason R. Pitarresi,[1,2,3] Maximilian Reichert,[1,2,3,6] Basil Bakir,[1,2,3] Shigetsugu Takano,[1,2,3] Janel L. Kopp,[7] Anja Wahl-Feuerstein,[5] Philip Hicks,[1,2,3] Maike Sander,[8] and Anil K. Rustgi [1,2,3,9]*

[1]Division of Gastroenterology, University of Pennsylvania, Philadelphia, Pennsylvania
[2]Department of Medicine, University of Pennsylvania, Philadelphia, Pennsylvania
[3]Abramson Cancer Center, University of Pennsylvania, Philadelphia, Pennsylvania
[4]Division of Gastroenterology, Department of Medicine, Washington University School of Medicine, St. Louis, Missouri
[5]Department of Medicine II, Medical Center, University of Freiburg, Freiburg, Germany
[6]II. Medizinische Klinik, Technical University of Munich, Munich, Germany
[7]Department of Cellular and Physiological Sciences, University of British Columbia, Vancouver, Canada
[8]Department of Pediatrics, Department of Cellular and Molecular Medicine, University of California San Diego School of Medicine, San Diego, California
[9]Department of Genetics, Perelman School of Medicine, University of Pennsylvania, Philadelphia, Pennsylvania

Background: The plasticity of pancreatic acinar cells to undergo acinar to ductal metaplasia (ADM) has been demonstrated to contribute to the regeneration of the pancreas in response to injury. *Sox9* is critical for ductal cell fate and important in the formation of ADM, most likely in concert with a complex hierarchy of, as yet, not fully elucidated transcription factors. **Results:** By using a mouse model of acute pancreatitis and three dimensional organoid culture of primary pancreatic ductal cells, we herein characterize the Ets-transcription factor *Etv5* as a pivotal regulator of ductal cell identity and ADM that acts upstream of *Sox9* and is essential for *Sox9* expression in ADM. Loss of *Etv5* is associated with increased severity of acute pancreatitis and impaired ADM formation leading to delayed tissue regeneration and recovery in response to injury. **Conclusions:** Our data provide new insights in the regulation of ADM with implications in our understanding of pancreatic homeostasis, pancreatitis and epithelial plasticity. *Developmental Dynamics 000:000–000, 2018.* © 2018 Wiley Periodicals, Inc.

Key words: Etv5; Sox9; pancreatitis; acinar ductal metaplasia

Submitted 19 November 2017; First Decision 22 February 2018; Accepted 8 March 2018; Published online 0 Month 2018

Introduction

Pancreatic organogenesis is orchestrated through a complex regulatory network during development, resulting in the formation of the endocrine and exocrine compartments. In turn, the exocrine compartment has two major lineages: acinar cell and ductal cell. The exocrine pancreas has limited proliferative capacity in the adult organism. However, in states of direct injury to acinar cells, there are adaptive responses that result in acinar and ductal regeneration through an intermediate acinar ductal metaplastic (ADM) state (Giroux and Rustgi, 2017; Puri et al., 2015). By utilizing recent advances in mouse models of pancreatitis and cell lineage labeling, a developing landscape of factors governing pancreatic regeneration is emerging (Lerch and Gorelick, 2013). It is proposed that stress, such as inflammation during pancreatitis, can foster cells to evolve into a de-differentiated state, making them vulnerable to changes in cell identity and transformation (Puri et al., 2015). It appears that the central component to this is the pancreatic acinar cell's unique capacity to undergo metaplasia to a ductal cell phenotype in the setting of acute pancreatitis.

Grant sponsor: NIH; Grant number: R01 DK060694; Grant sponsor: NIH/NIDDK; Grant numbers: T32-DK007066, NIH-F32CA136124, NIH-R21CA194839, NIH-R01 DK078803; Grant sponsor: National Pancreas Foundation; Grant sponsor: Deutsche Krebshilfe; Grant number: 110037; Grant sponsor: Max Eder Program; Grant numbers: 111273, 110972; Grant sponsor: AGA-Actavis Research Award in Pancreatic Disorders; Grant sponsor: NIH/NIDDK P30-DK050306 Center for Molecular Studies in Digestive and Liver Diseases; Grant sponsor: American Cancer Society; Grant number: RP-10-033-01-CCE.

†These authors contributed equally to this work.

ABBREVIATIONS: 3D, three-dimensional; ADM, acinar ductal metaplasia Egf epidermal growth factor; BSA, bovine serum albumin; DAPI, 4′,6-diamidine-2-phenylidole-dihydrochloride DBS *Dolichos biflorus* agglutinin; EDTA, ethylenediaminetetraacetic acid; EGFR, epidermal growth factor receptor; EMT, epithelial–mesenchymal transition; FACS, fluorescence-activated cell sorting; FITC, fluorescein isothiocyanate; H&E, hematoxylin and eosin; IF, immunofluorescence; IHC, immunohistochemistry; PanIN, pancreatic intraepithelial neoplasia; PDAC, pancreatic ductal adenocarcinoma; PDC, pancreatic ductal cell; PFA, paraformaldehyde; qPCR, quantitative polymerase chain reaction; TUNEL, terminal deoxynucleotidyl transferase–mediated deoxyuridine triphosphate nick-end labeling YFP yellow fluorescent protein

*Correspondence to: Anil K. Rustgi, T. Grier Miller Professor of Medicine & Genetics, Tumor Biology Program, Abramson Cancer Center, 900 Biomedical Research Building II/III, University of Pennsylvania, 415 Curie Blvd., Philadelphia, PA 19104. E-mail: anil2@mail.med.upenn.edu

Article is online at: http://onlinelibrary.wiley.com/doi/10.1002/dvdy.24626/abstract

ADM may represent reprogramming of a progenitor population, direct transdifferentiation of acinar cells to ductal cells, or transdifferentiation by means of an intermediate cell type (Reichert and Rustgi, 2011). In addition to a ductal morphology, ADM cells co-express acinar and ductal markers and exhibit up-regulation of signaling pathways such as epidermal growth factor receptor (EGFR) and NOTCH, and downstream effectors such as the KRAS-MEK-MAPK pathway, which are increased during pancreatic tumorigenesis (Miyamoto et al., 2003; Thayer et al., 2003; Ardito et al., 2012; Collins et al., 2014).

Key pancreatic transcriptional factors have been identified that govern endocrine (*Pdx1*) and exocrine cell lineage fates for acinar cells (*Ptf1a* and *p48*) or ductal cells (*Sox9, Hnf1β, Hnf6*, and *Prrx1*) (Reichert and Rustgi, 2011). Of interest, the loss of acinar markers such as *Ptf1a* (Krah et al., 2015) and Mist1a (Pin et al., 2001), or overexpression of the ductal marker *Sox9* (Kopp et al., 2012; Prevot et al., 2012) in the acinar compartment results in spontaneous ADM. Transcriptional factors that regulate convergence on ductal cell fate have remained elusive apart from *Sox9, Prrx1, Hnf1β, and Hnf6* (Jacquemin et al., 2000, 2003; Haumaitre et al., 2005; Pierreux et al., 2006; Seymour et al., 2007; Reichert et al., 2013a). The *Sox9* transcription factor has been shown to annotate pancreatic embryonic ductal cells that are multipotent (Kopp et al., 2011). While the ectopic induction of *Sox9* ($Ptf1a^{Cre};Sox9^{OE}$) was shown to significantly increase the development of ADM in the setting of pancreatitis, the acinar loss of Sox9 ($Ptf1a^{CreER};Sox9^{fl/fl}$) was associated with continued development of ADM (Kopp et al., 2012). Several recent studies have shown that the key to preventing tumorigenesis is in the maintenance of acinar cell identity. In concert with mutant $Kras^{G12D}$, *Sox9* accelerates the progression of ADM to pancreatic intraepithelial neoplasia (PanIN) (Kopp et al., 2012). Thus, it is important to elucidate how Sox9 is regulated especially in the context of ADM, known to be a precursor to PanIN. To that end, we have demonstrated previously that *Prrx1* functionally activates the *Sox9* promoter, although there are likely other factors important in its regulation (Reichert et al., 2013a).

In an effort to identify additional transcriptional factors that may serve as "drivers" of ADM, the transcriptional profile of cells derived from embryonic progenitor cells (which may represent potential embryonic ductal cells), pancreatitis injury/regeneration (ADM), and early neoplasia (PanIN) were analyzed. Strikingly elevated levels of the Ets-transcriptional factors ETV1 and ETV5 were observed in these three processes (Reichert et al., 2013a). Ets factors are characterized by their conserved helix-turn-helix binding motif (Ets domain), which binds to the GGAA/T core consensus sequence (Kar and Gutierrez-Hartmann, 2013). Approximately 30 Ets factors have been classified into 9 subfamilies, with *ETV1* and *ETV5* belonging to the PEA3 subfamily (Oh et al., 2012). These factors are known downstream targets of *Kras* (mutated in $>90\%$ of human pancreatic ductal adenocarcinoma (PDAC)) and have been implicated in numerous cellular processes including proliferation, senescence, apoptosis, and differentiation (Kar and Gutierrez-Hartmann, 2013). In development, the PEA3 family of Ets transcription factors has been observed in organs that undergo branching morphogenesis such as the lung, salivary gland, and pancreas. Notably, ETV5 has been preferentially observed to be expressed in the developing epithelial buds and ETV1 found in the mesenchymal compartment, indicating a potential role for these factors in epithelial–mesenchymal plasticity (Chotteau-Lelievre et al., 2003; Kobberup et al., 2007). Given its distinct epithelial expression in branching morphogenesis in the developing pancreas, we sought to examine the role of *Etv5* in ductal morphogenesis and regeneration in pancreatitis.

Herein we define novel functional roles for *Etv5* in the regulation of ADM and pancreatic regeneration in concert with *Sox9*. To examine *Etv5* in inflammation and regeneration, we used *Pdx1cre;* $Etv5^{fl/fl};Rosa^{YFP}$ and $Pdx1cre;Rosa^{YFP}$ mice and cell lines derived from these animals grown in three-dimensional (3D) organoid culture. The conditional loss of *Etv5* was associated with significantly more severe pancreatitis, impaired regeneration, and a significant reduction in ADM. ETV5 was found to be required for hollow lumen formation in 3D organoid culture, a hallmark of ductal cell fate. Finally, we identified *Sox9* as a novel downstream regulator of *Etv5* through immunofluorescence co-localization in ADM in vivo and luciferase promoter assay.

Results

Etv5 is Critical for Regeneration From Cerulein Induced Acute Pancreatitis In Vivo

Given the previously well described roles of *Etv1* and *Etv5* in organs undergoing branching morphogenesis (Chotteau-Lelievre et al., 2003) and the expression of ETV5 in the developing pancreatic epithelial bud (Kobberup et al., 2007), we sought first to evaluate the expression of ETV5 in the normal adult mouse pancreas. We found sustained expression of ETV5 primarily in the ductal compartment of the normal adult pancreas, with noted increased expression in PanIN lesions in $Pdx1\text{-}cre;LSL\text{-}Kras^{G12D}$ mice (Fig. 1A). A previously generated conditional knockout of *Etv5* (Zhang et al., 2009), was bred with mice with the pancreatic specific promoter, *Pdx1-cre* (Gu et al., 2002) and $Rosa26^{YFP}$ (Srinivas et al., 2001). The presence of yellow fluorescent protein (YFP) expression allows independent verification of recombination efficiency and serves as a lineage label.

$Pdx1cre;Etv5^{fl/fl};Rosa26^{YFP}$ mice aged to 3, 6, and 12 months did not demonstrate any disruption in pancreatic ductal architecture or other apparent phenotype (Fig. 1C). Based on these data, it appeared that ETV5 is not required under homeostatic conditions, but we sought to investigate its role during injury and regeneration. We have previously examined the transcriptional profile of cells derived from embryonic progenitor cells, pancreatitis injury/regeneration (ADM), and early neoplasia (PanIN) and found strikingly elevated levels of the Ets-transcriptional factor Etv5 in these three processes (Reichert et al., 2013a). Given these findings and previous data demonstrating the important role of *Etv5* in ductal development (Kobberup et al., 2007), we sought to evaluate how the loss of *Etv5* would affect response to inflammation and subsequent regeneration.

We used a well-established model of cerulein induced pancreatitis (Lerch and Gorelick, 2013) where acinar cell injury is rapidly induced (day 1) after intraperitoneal cerulein administration, followed by the emergence of ADM structures (day 3), and inflammatory cellular infiltration and stromal edema, all characteristic features of acute pancreatitis. Subsequently, there is a recovery phase with regeneration of epithelial cells and resolution of the inflammation by day 7. We examined cohorts of age-matched littermates of $Pdx1cre;Etv5^{WT/WT};Rosa26^{YFP}$, $Pdx1cre;Etv5^{fl/WT};Rosa26^{YFP}$, and $Pdx1cre;Etv5^{fl/fl};Rosa^{YFP}$ mice on 1, 3, 7, and 21 days after induction of pancreatitis with cerulein (Fig. 1B).

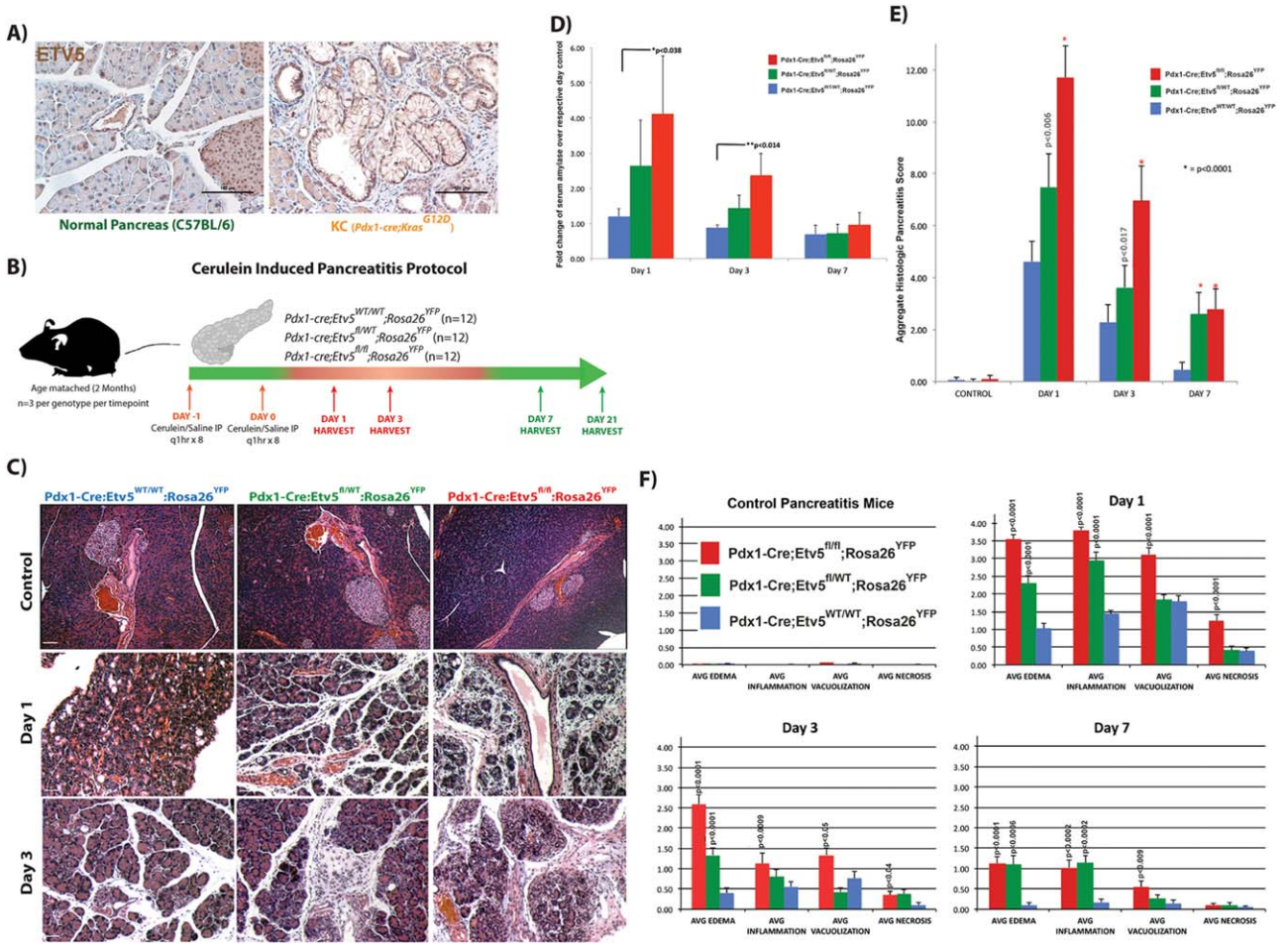

Fig. 1. *Etv5* is critical for regeneration from cerulein induced acute pancreatitis. **A**: ETV5 immunohistochemistry in mouse sections with the indicated genotypes. Expression of ETV5 is restricted to the ductal compartment in the normal adult pancreas. PanIN lesions display elevated levels of ETV5. Scale bar = 100 μM. **B**: Schematic experimental design of cerulein induced acute pancreatitis. Three mice per genotype were killed and pancreata were harvested on day 1, 3, 7, and 21 after cerulein injection. Seven randomly selected high power fields of the pancreata from each of the sacrificed mice were examined for demonstrated analyses. **C**: The severity of acute cerulein induced pancreatitis is significantly increased in *Pdx1cre;Etv5$^{fl/WT}$;Rosa26^{YFP}* and *Pdx1cre;Etv5$^{fl/fl}$;Rosa^{YFP}* mice in comparison to *Pdx1cre;Etv5$^{WT/WT}$;Rosa^{YFP}* mice. Histology of saline injected control as well as cerulein injected mice at day 1 and day 3 after cerulein injection. Loss of one and, to an even greater extent, two alleles of *Etv5* is associated with significantly more severe pancreatitis. **D**: Quantification of fold change of serum amylase at day 1, 3, and 7 after cerulein injection against respective day controls. *P* values calculated with student's two-sided *t*-test. **E,F**: Aggregate (E) and component (F) histologic grading for edema, inflammation, vacuolization and necrosis in mice with the depicted genotype after saline injection and day 1, 3, and 7 after cerulein injection, respectively. The loss of *Etv5* is associated with significantly more severe pancreatitis at day 1 and 3, and impaired regeneration at day 7 after cerulein administration.

In our control cohort of *Pdx1cre;Etv5$^{WT/WT}$;Rosa26^{YFP}* mice we observed maximal inflammation on day 1 with prominent ADM development on day 3 followed by full regeneration on day 7 (Fig. 1C,E,F). The loss of a single allele of *Etv5* (*Pdx1cre;Etv5$^{fl/WT}$;Rosa26^{YFP}*) was associated with significantly more severe histologic pancreatitis on days 1, 3, and 7 (Fig. 1C,E). Using a previously validated histologic scoring system (Rongione et al., 1997) graded by two blinded, independent reviewers, with the loss of a single allele of Etv5 we observed significantly more severe edema and inflammation on day 1 and 7 and significantly more edema on day 3 (Fig. 1F). Compared with control mice, the complete loss of Etv5 (*Pdx1cre;Etv5$^{fl/fl}$;Rosa^{YFP}*) was associated with an even greater degree of histologic pancreatitis on days 1, 3, and 7 (Fig. 1C,E,F). Specifically, there was significantly more severe edema, inflammation, and vacuolization on days 1, 3, and 7 and more severe necrosis on days 1 and 3 in the *Pdx1cre;Etv5$^{fl/fl}$;Rosa^{YFP}* animals. Histology examined from a separate cohort of animals from wild-type and *Pdx1cre;Etv5$^{fl/fl}$;Rosa^{YFP}* mice 21 days after initiation of pancreatitis demonstrated normalization of histology in all groups, suggesting a delay but not total impairment of acinar and ductal regeneration (Fig. 2D).

We examined both serum amylase as well as relative immunofluorescence staining for amylase to quantify the severity of pancreatitis. Serum amylase from *Pdx1cre;Etv5$^{fl/fl}$;Rosa^{YFP}* animals from days 1 and 3 of the protocol was four-fold and 2.5-fold higher than respective controls (Fig. 1D). Using immunofluorescence for quantified amylase area, we found a stepwise, significantly more severe pancreatitis (correlating with lower amylase area/DAPI [4′,6-diamidine-2-phenylidole-dihydrochloride] area) in *Pdx1cre;Etv5$^{fl/WT}$;Rosa26^{YFP}* and *Pdx1cre;Etv5$^{fl/fl}$;Rosa^{YFP}* mice in comparison to controls on days 1 and 3 (Fig. 2A). On day 7, when control mice demonstrated normal regeneration of the

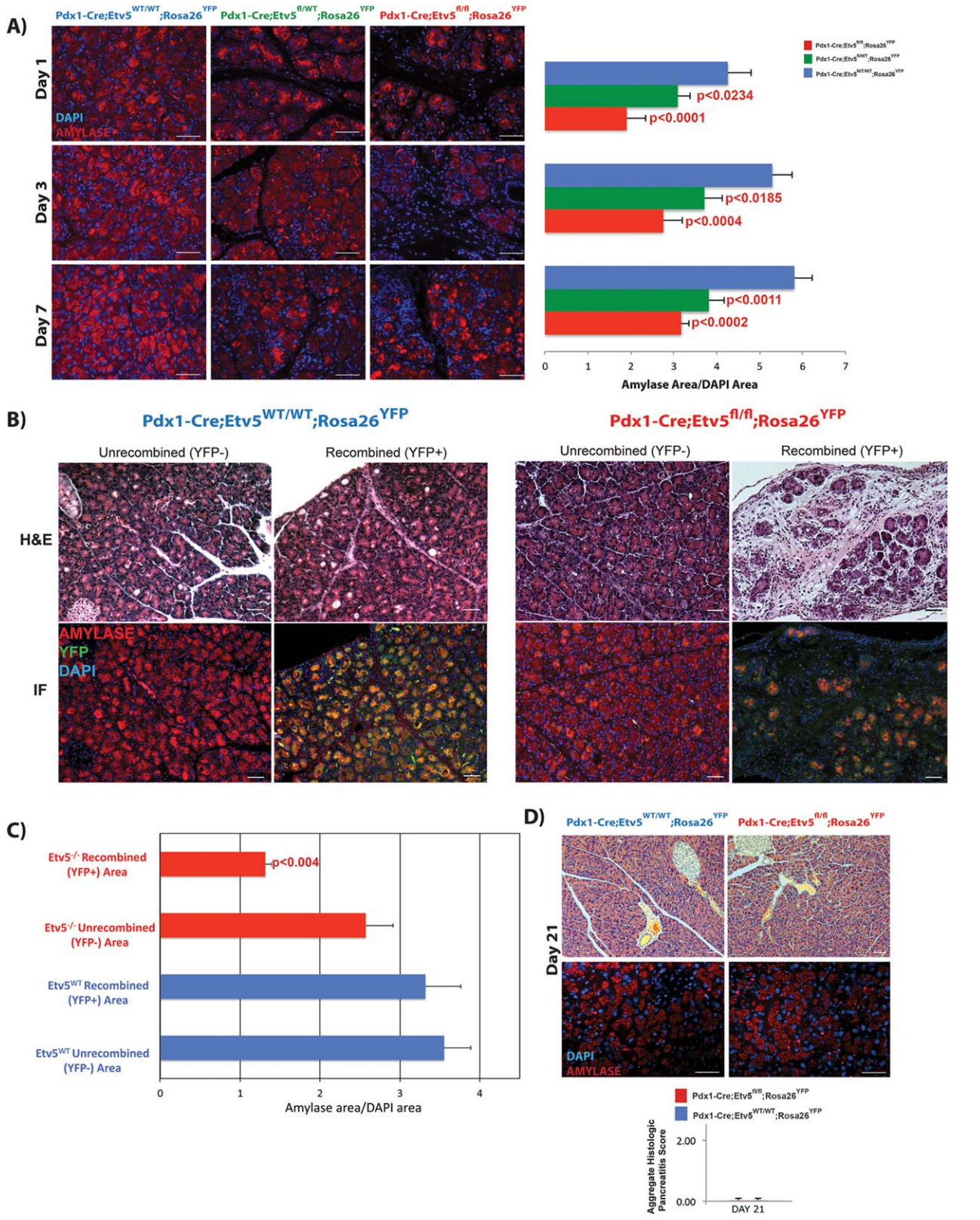

Fig. 2. The loss of *Etv5* is associated with delayed regeneration from cerulein induced acute pancreatitis. **A**: Immunofluorescence staining for amylase in mice with the indicated genotypes at day 1, 3, and 7 after cerulein injection and analysis of the amylase positive area relative to DAPI. The amylase positive area is significantly decreased in mice with loss of *Etv 5* compared with wild-type. Scale bar = 50 μM. **B,C**: Immunofluorescence staining (B) and quantification (C) for amylase and YFP in *Pdx1cre;Etv5$^{WT/WT}$;Rosa26^{YFP}*, and *Pdx1cre;Etv5$^{fl/fl}$;Rosa^{YFP}* mice. Amylase expression in paired YFP + (recombined) and YFP- (unrecombined) areas within the same animal on day 3 after cerulein induced pancreatitis. While YFP + and YFP- areas are similar in *Pdx1cre;Etv5$^{WT/WT}$;Rosa26^{YFP}* mice, in *Pdx1cre;Etv5$^{fl/fl}$;Rosa^{YFP}* mice there is significantly more loss of amylase expression in the YFP + areas in comparison to the YFP- areas. Two mice for each genotype were examined. Scale bar = 50 μM. **D**: Histologic normalization of pancreata at 21 days after induction of cerulein induced pancreatitis with and without the loss of *Etv5*. Immunofluorescence staining for amylase was also performed between *Pdx1cre;Etv5$^{WT/WT}$;Rosa26^{YFP}* and *Pdx1cre;Etv5$^{fl/fl}$;Rosa^{YFP}* mice. Three mice were examined for each genotype.

acinar compartment, there was continued significant loss of amylase area in *Pdx1cre;Etv5$^{fl/WT}$;Rosa26^{YFP}* and *Pdx1cre;Etv5$^{fl/fl}$;Rosa^{YFP}* mice which normalized by day 21 (Fig. 2A,D).

Examination of *Pdx1cre;Etv5$^{WT/WT}$;Rosa26^{YFP}* and *Pdx1cre;Etv5$^{fl/fl}$;Rosa^{YFP}* mice demonstrated no significant difference in terminal deoxynucleotidyl transferase–mediated deoxyuridine triphosphate nick-end labeling (TUNEL) staining for apoptosis (data not shown). While the vast majority (>70–80%) of the pancreata of animals expressed YFP, there was a minority of areas that were YFP-negative (YFP-), and thus, unrecombined. Comparing *Pdx1cre;Etv5$^{fl/fl}$;Rosa^{YFP}* animals with control animals, we examined amylase expression in paired YFP + (recombined) and YFP- (unrecombined) areas within the same animal on day 3 of the pancreatitis protocol (Fig. 2B,C). While amylase expression in the YFP + and YFP- areas of control wild-type *Etv5* animals was similar, YFP + areas in *Pdx1cre;Etv5$^{fl/fl}$;Rosa^{YFP}* animals demonstrated significantly more loss in amylase than in corresponding YFP- areas within the same mouse (Fig. 2C). Taken together, these data demonstrate that Etv5 is found in normal pancreatic ducts and its loss is likely critical in mediating regeneration from acute pancreatitis.

Delayed Recovery From Acute Pancreatitis With Etv5 Loss is Associated With Impaired ADM Formation

Given our findings of impaired regeneration in response to pancreatitis in mice with conditional loss of *Etv5*, we next sought to examine whether Etv5 loss was associated with a change in the development of ADM. ADM was quantified by immunofluorescence as DAPI positive structures that concurrently expressed both the ductal marker K19 and the acinar marker amylase (Reichert and Rustgi, 2011; Reichert et al., 2013a) These structures were concurrently confirmed histologically on serial sections. As expected, in saline injected *Pdx1cre;Etv5$^{WT/WT}$;Rosa26^{YFP}* and *Pdx1cre;Etv5$^{fl/fl}$;Rosa^{YFP}* mice, the histology of the acinar and ductal compartments was normal, with no ADM apparent (Fig. 3A,B, top panels). By contrast, *Pdx1cre;Etv5$^{WT/WT}$;Rosa26^{YFP}* with cerulein induced pancreatitis displayed ADM formation by day 3 after injection (Fig. 3A, left lower panel). To analyze the frequency of ADM in *Pdx1cre;Etv5$^{fl/fl}$;Rosa^{YFP}* animals, we identified a separate cohort of *Pdx1cre;Etv5$^{WT/WT}$;Rosa26^{YFP}* animals (n = 3 mice per time point) that had undergone cerulein induced pancreatitis which resulted in a histologically matched degree of inflammation and pancreatitis as was observed in the *Pdx1cre;Etv5$^{fl/fl}$;Rosa^{YFP}* mice (Fig. 3A, lower left panels; 3B,lower panels). Among these animals with a similar degree of inflammation, the loss of *Etv5* was associated with a four-fold decrease in ADM lesions compared with their wild-type controls (Fig. 3B, bottom panel). Thus, *Etv5* may play a role in ADM formation, resulting in delayed tissue regeneration.

Etv5 is Associated With Sox9 and ADM Formation In Vivo

Given the striking reduction in ADM associated with *Etv5* loss, we sought to examine the association between *Etv5* and factors governing ADM formation. It has been demonstrated that *Sox9* plays a crucial role in the formation and maintenance of ADM (Kopp et al., 2012; Prevot et al., 2012). Therefore, we evaluated the relationship of *Sox9* and *Etv5* during acute pancreatitis. We first examined pancreata from wild-type mice undergoing acute cerulein induced pancreatitis that were *Dolichos biflorus* agglutinin (DBA) lectin sorted for the ductal cell compartment, which contains cells that have undergone ADM (Reichert et al., 2013b). Among these cells, we found a significant four- to five-fold increase of *Etv5* and *Sox9* gene expression at day 3 in comparison to day 1 (Fig. 3C).

We next examined *Etv5* in wild-type tissue from mice with acute pancreatitis and found by immunofluorescence (IF) that ETV5 and SOX9 co-localize in ADM in acute pancreatitis (Fig. 3D). To examine the effects of the loss of *Etv5* upon SOX9 in ADM, we then examined *Pdx1cre;Etv5$^{fl/fl}$;Rosa^{YFP}* mice undergoing pancreatitis. In these animals, the loss of *Etv5* in the few ADM that were present was associated with the loss of SOX9 as well (Fig. 3E). Finally, to examine the effect of the loss of *Sox9* on Etv5 in pancreatitis and ADM, we examined *Ptf1a^{CreER};Sox9$^{fl/fl}$;Rosa^{YFP}* mice that underwent a cerulein induced pancreatitis protocol (Kopp et al., 2012). In these mice, ADM frequency was robust and while SOX9 was absent in ADM, ETV5 remained present in the ADM (Fig. 3F). Thus, these data suggest a spatial and temporal association of ETV5- and SOX9-expression in the context of acute pancreatitis. ETV5 is expressed early in conjunction with Sox9 after the induction of pancreatitis, it co-localizes with SOX9 in ADM, is required for SOX9 expression in ADM, but is not lost in the context of *Sox9* deletion, suggesting that *Etv5* may be potentially upstream of *Sox9*.

Etv5 is Required for Hollow Lumen Formation in Pancreatic Ductal Cell Organoids

To elucidate further the mechanism by which *Etv5* may affect ductal metaplasia, we sought to examine the role of ETV5 in primary pancreatic ductal cells (PDCs) in 3D organoids in vitro. We have described previously the technique for the isolation and propagation of primary pancreatic ductal cells and their growth in 3D organoids (Reichert et al., 2013b). Early passage PDCs were suspended in a mix of collagen I and medium and seeded on a solidified layer of collagen I (Reichert et al., 2013b). Using this system, wild-type PDCs form round 3D cysts with a hollow lumen surrounded by a layer of single cells within 24–48 hr of seeding (Fig. 4C). Using lentiviral transfection, we over-expressed ETV5 in PDCs and validated this by both Western blot and quantitative polymerase chain reaction (qPCR) (Fig. 4A,B). Identically seeded PDC mEtv5 cells grown in organoid culture in parallel with parental controls demonstrated significantly enhanced cyst/hollow lumen formation within 48 hr of seeding, a hallmark of ductal cell fate (Fig. 4C,D).

Next, we isolated PDCs from *Etv5$^{fl/fl}$;Rosa^{YFP}* mice and performed in vitro lentiviral Cre recombination (PDC m*Etv5$^{fl/fl}$;Rosa^{YFP}* and PDC m*Etv5$^{fl/fl}$;Rosa^{YFP};LV-Cre*). After successful transfection we performed fluorescence-activated cell sorting (FACS) sorting for YFP to enrich for successfully recombined cells (Fig. 4A,B). Comparing PDC m*Etv5$^{fl/fl}$;Rosa^{YFP}* and PDC m*Etv5$^{fl/fl}$;Rosa^{YFP};LV-Cre* grown in 3D organoid culture, Etv5 loss abrogated the capacity of the ductal cells to form regular hollow lumens (Fig. 4E,F). By contrast, we have shown previously that ETV1 overexpression in 3D organoid culture is associated with loss of epithelial polarity, spindle-shaped morphology, and the induction of key regulators of epithelial–mesenchymal transition (EMT) (Heeg et al., 2016). It is striking that these two, highly related transcription factors, *Etv1* and *Etv5*, with distinct mesenchymal and epithelial roles in pancreatic development, appear to

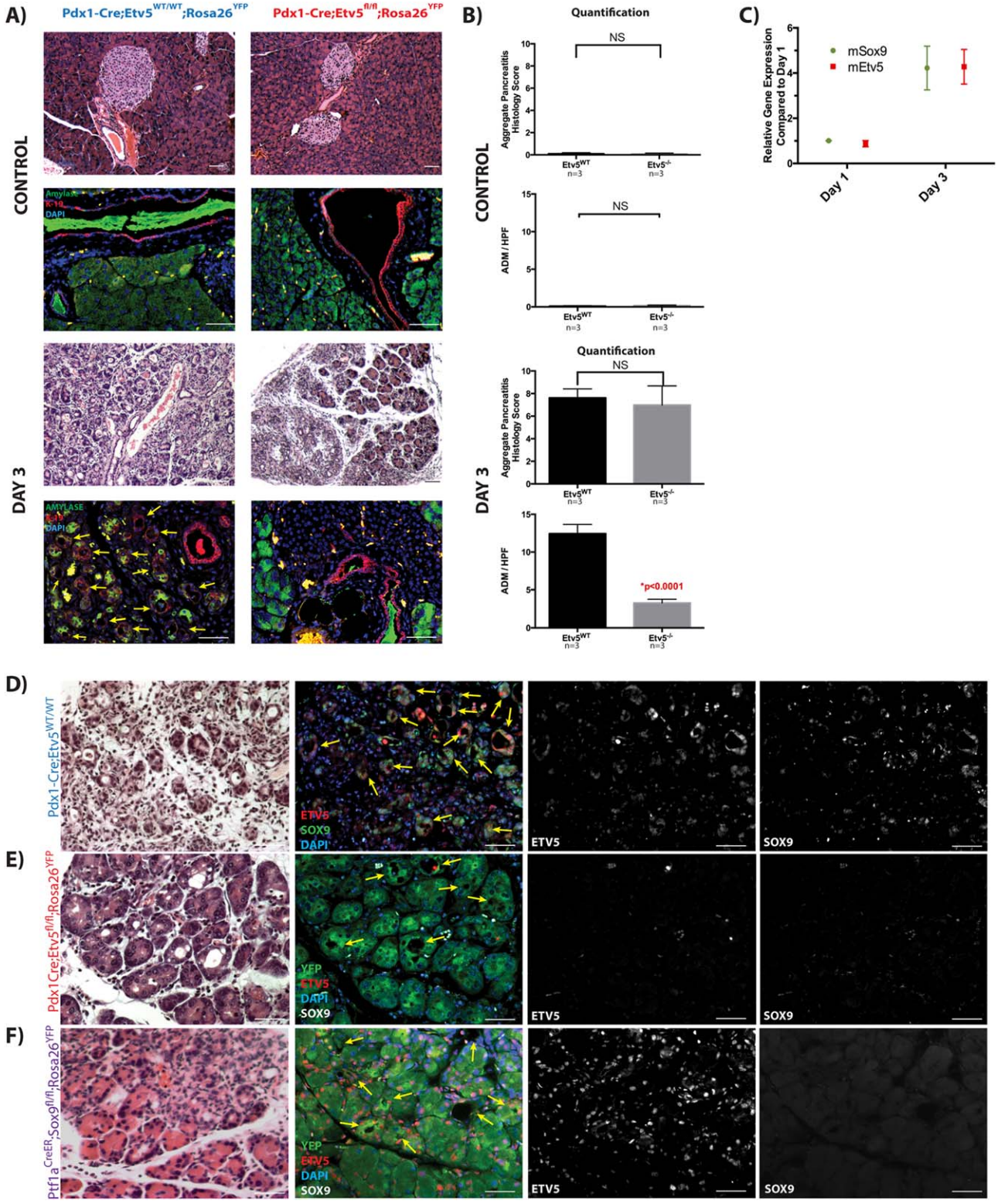

Fig. 3. Loss of Etv5 is associated with impaired acinar to ductal metaplasia (ADM) formation. **A,B**: *Pdx1cre;Etv5$^{fl/fl}$;Rosa^{YFP}* animals with saline or cerulein injection were matched to a cohort of *Pdx1cre;Etv5$^{WT/WT}$;Rosa26^{YFP}* animals with a histologically identical degree of inflammation and pancreatitis (three mice per genotype and day analyzed, seven high power fields per animal). Immunofluorescence for K19 and Amylase and quantification of ADMs at day 3 after saline or cerulein injection was performed. ADMs are characterized by concurrent expression of K19 and Amylase. Loss of Etv5 is associated with a significant reduction of ADMs (B, bottom panels). **C**: Expression of Sox9 and Etv5 by qPCR in DBA lectin positive sorted cells at day 1 and 3 after cerulein induced pancreatitis. Expression of SOX9 and ETV5 is significantly increased at day 3. **D**: Immunofluorescence staining for ETV5 and SOX9 in *Pdx1cre;Etv5$^{WT/WT}$* mice at day 3 after cerulein induced pancreatitis. ETV5 and SOX9 co-localize in ADM in acute pancreatitis. In aggregate, approximately 80% of the colocalization was noted in association with ADM related structures. **E**: Immunofluorescence staining for ETV5, SOX9, and YFP in *Pdx1cre;Etv5$^{fl/fl}$;Rosa^{YFP}* mice at day 3 after cerulein induced pancreatitis. Loss of *Etv5* is associated with the loss of SOX9 in ADMs. **F**: Immunofluorescence staining for ETV5, SOX9, and YFP in *Ptf1a^{CreER};Sox9$^{fl/fl}$;Rosa^{YFP}* mice at day 2 after cerulein induced pancreatitis. ETV5 remains present in the ADM despite the loss of *Sox9*. Scale bar = 50 μM. Yellow Arrows indicate ADM.

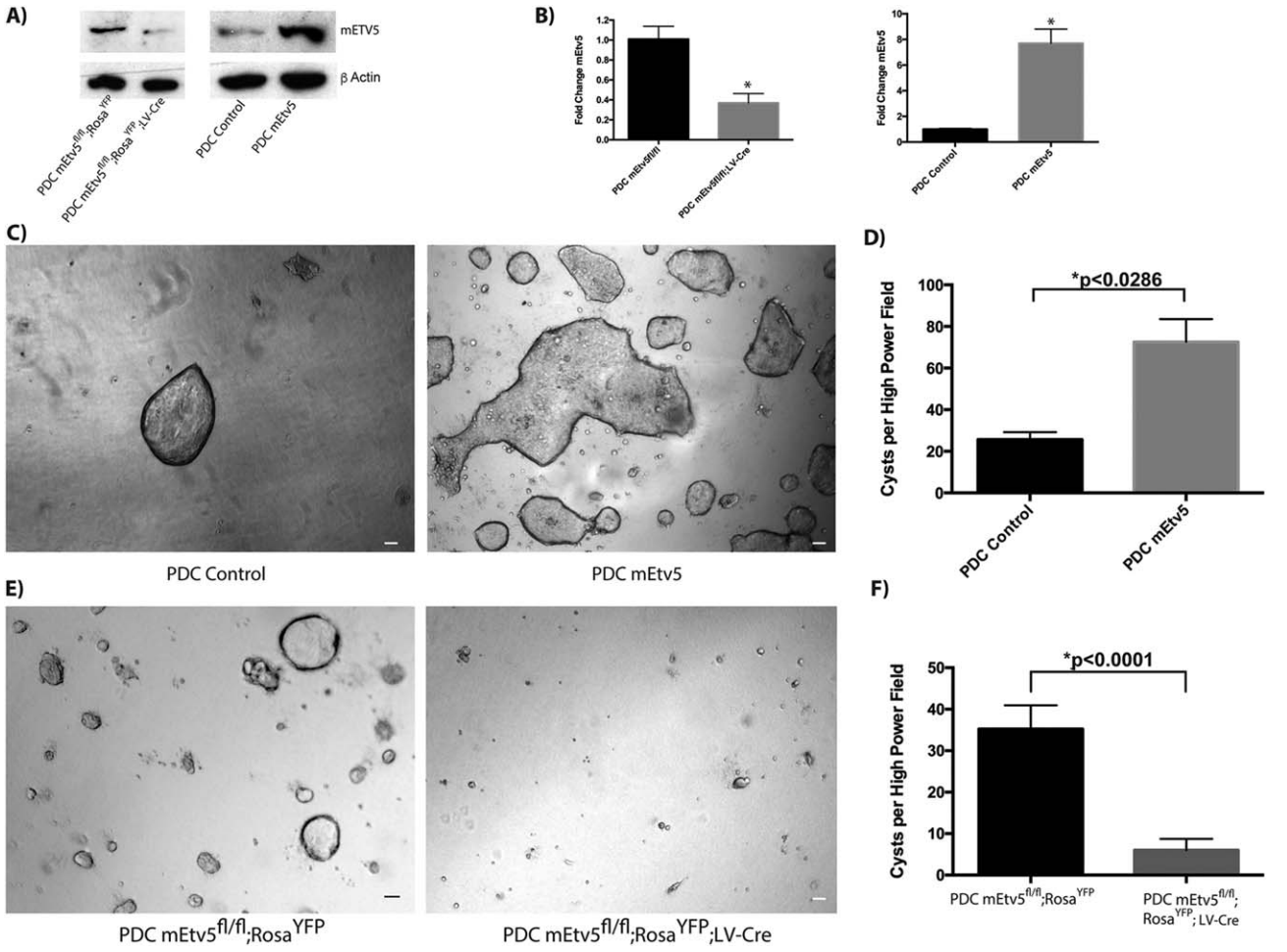

Fig. 4. Etv5 is required for hollow lumen formation in pancreatic ductal cell organoids. **A**: Western blot for Etv5 in the control and experimental PDC cell lines used. ß-Actin served as loading control. **B**: Left panel: RT-qPCR for ETV5 in PDCs isolated from *Etv5*$^{fl/fl}$;*Rosa*^{YFP} mice transduced with control (bar 1) and LV-*Cre* (bar 2). Etv5 is significantly reduced after *Cre* transduction. Right panel: RT-qPCR for ETV5 in PDCs isolated from wild-type mice transduced with control (bar 1) and Etv5 (bar 2). Etv5 is significantly increased after Etv5 transduction. **C**: Representative examples of 3D organoids of primary PDCs isolated from *Pdx1cre;Etv5*$^{WT/WT}$ mice. **D**: ETV5 overexpression leads to significantly enhanced cyst formation within 48 hr after seeding. **E**: Representative examples of 3D organoids of primary PDCs isolated from *Etv5*$^{fl/fl}$;*Rosa*^{YFP} mice. **F**: Loss of *Etv5* after transduction with lentiviral Cre significantly reduces cyst formation capacity of the pancreatic ductal cells. Bar graphs represent the mean cyst number per high power field of 3 independent experiments with SEM. Scale bar = 50 μM.

have reminiscent roles in inducing mesenchymal and ductal cell identities in fully differentiated pancreatic ductal cells.

Etv5 is Associated With Sox9 in its Role in Hollow Lumen Formation in Pancreatic Duct Cell Organoids

To examine the downstream factors associated with this striking phenotype, we performed a screen of ductal and acinar markers on PDCs overexpressing ETV5 grown in organoid culture. We found a significant down-regulation of acinar markers PTF1a and MIST1 and a significant seven-fold increase in SOX9 (Fig. 5A). To evaluate this relationship, we performed IF from cysts of PDCs overexpressing ETV5 grown in organoid culture. Co-localization of ETV5 and SOX9 was found particularly in areas of cyst fusion (Fig. 5B).

In silico screening demonstrated several putative Ets binding sites upstream of the *Sox9* promoter (Fig. 5C). We generated a *Sox9* luciferase reporter gene construct that contains a portion of the *Sox9* promoter with these Ets binding sites (Fig. 5C). ETV5 overexpression significantly increased *Sox9* luciferase activity in comparison to the pGL3-control vector (Fig. 5D). In combination with IF co-localization of Sox9 and Etv5 in ADM (Fig. 3D) and in 3D organoids (Fig. 5B), these data suggest a novel and exciting potential regulation of *Sox9* by ETV5.

Discussion

Pancreatic ductal cell differentiation is regulated tightly in the context of development and regeneration after injury. Using a well-established model of cerulein-induced pancreatitis in genetically engineered mice and 3D organoid culture, we now define a novel role for the Ets-transcription factor *Etv5* in the regulation of ductal identity, ADM, and pancreatic regeneration in conjunction with *Sox9*.

Ets-transcription factors of the PEA3-family, namely *Etv1* and *Etv5*, display a distinct expression pattern during the development of organs that undergo branching morphogenesis, including the pancreas. Branching morphogenesis requires a well-

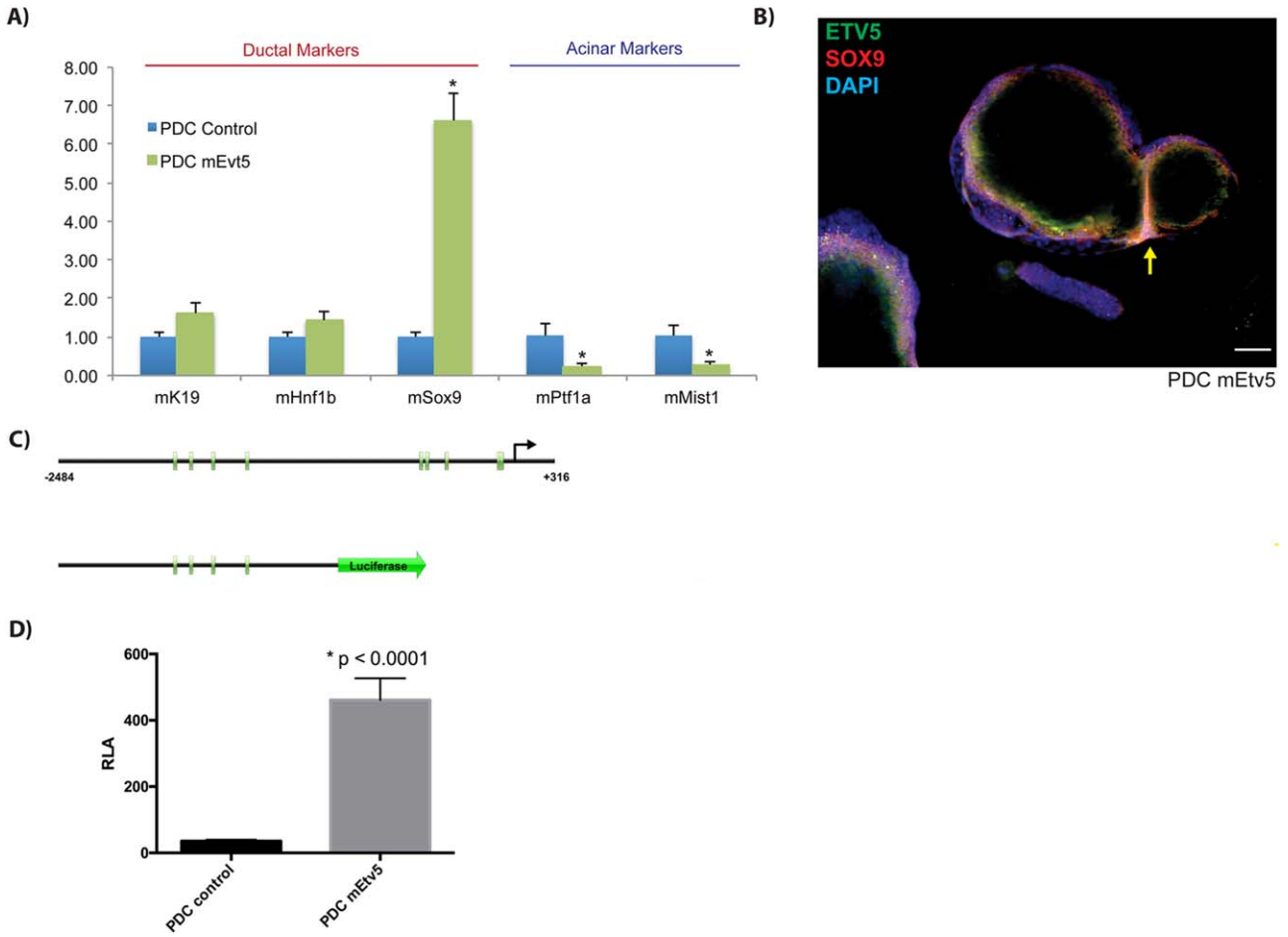

Fig. 5. Etv5 is associated with Sox9 in its role in hollow lumen formation in PDC organoids. **A**: Expression of ductal and acinar lineage markers in normal and ETV5 overexpressing PDCs. ETV5 overexpression is associated with significantly reduced expression of acinar markers while expression of SOX9 is significantly increased. $^{*}P < 0.001$. **B**: Immunofluorescence staining for ETV5 and SOX9 in 3D organoids of PDCs overexpressing ETV5. ETV5 and SOX9 co-localize, particularly in sites of cyst fusion (arrow). **C**: Schematic diagram of the Sox9 promoter. Green boxes indicate predicted ETV5 binding sites. **D**: Luciferase reporter assay of the *Sox9* promoter. *Sox9* promoter activity is significantly increased in ETV5 overexpressing PDCs compared with control. Bar graphs represent three independent experiments with SEM, Scale bar = 50 μM.

orchestrated interaction of epithelial and mesenchymal tissue compartmental factors. While expression of *ETV1* is restricted to the mesenchymal compartment, *ETV5* is highly expressed in the growing epithelial buds, suggesting that *Etv5* may play an important role for epithelial differentiation and, ultimately, ductal cell identity (Yuen et al., 2011). We have demonstrated that *Etv1* is critical in the mesenchymal expansion and the desmoplastic stromal response to pancreatic cancer, in association with downstream targets of SPARC and HAS2 (Heeg et al., 2016).

Here, we demonstrate that ETV5 overexpression in 3D organoid culture fosters exuberant cyst/lumen formation, a hallmark of ductal cell fate in 3D organoid culture, and the ablation of *Etv5* abrogates this process (Fig. 4E,F). In contrast, we have previously demonstrated that ETV1 overexpression in identical 3D organoid culture is associated with loss of epithelial polarity, spindle-shaped morphology, and the induction of key regulators of EMT (Heeg et al., 2016). Thus, *Etv1* and *Etv5* induce mesenchymal and ductal cell fates in fully differentiated pancreatic ductal cells highly reminiscent of their distinct mesenchymal and epithelial roles in pancreatic development.

The plasticity of pancreatic acinar cells in their capacity to undergo ADM in the setting of acute pancreatitis may serve as a transition point to develop PanIN as well as the normal homeostatic regeneration of the injured acinar and ductal compartments. Unlike many other organs, the pancreas is not known to have a readily identifiable adult stem cell population to regenerate in the setting of injury, rather, acinar cells undergo ADM after injury, perhaps underscoring the presence of facultative progenitor cells. Elegant mouse studies have demonstrated the loss of traditional acinar markers, like *Mist1* (Shi et al., 2012) or *Ptf1a* (Krah et al., 2015), or the overexpression of the ductal marker *Sox9* (Kopp et al., 2012) is sufficient to initiate the development of ADM. Ductal regulatory genes such as *Pdx1* and *Sox9* are re-expressed during ADM but the specific mechanisms triggering ADM are not understood (Pin et al., 2015).

We found that the conditional loss of *Etv5* (*Pdx1cre;Etv5$^{fl/fl}$;Rosa^{YFP}*) is associated with significantly more severe, acute pancreatitis and delayed recovery, indicating an important role for *Etv5* in the tissue homeostasis of the exocrine pancreas. Cells that have undergone ADM after injury through pancreatitis recover rapidly and provide an adaptive mechanism of tissue regeneration (Reichert and Rustgi, 2011). Strikingly, we found that *Pdx1cre;Etv5$^{fl/fl}$;Rosa^{YFP}* animals developed ADMs at a significantly lower frequency than wild-type controls exposed to a

similar degree of pancreatitis. Taken together, our findings suggest that *Etv5* might play a role in ADM formation and that the loss of *Etv5* could impair ADM formation resulting in delayed tissue regeneration.

ADM is believed to be triggered by a combination of inflammatory factors that include JAK/STAT signaling, IL6/IL6R, and Yap1/Taz, as well as signaling pathways influenced by EGFR, Notch and Ras (Pin et al., 2015; Gruber et al., 2016). In fact, ADM is a prominent feature in genetic mouse models in which Ras or PI3K, downstream of Ras, are highly elevated (Ji et al., 2009; Payne et al., 2015). Importantly, the PEA3 family of Ets transcription factors, including Etv5, are known downstream targets of RAS (Kar and Gutierrez-Hartmann, 2013). As we demonstrate that *Etv5* is crucial in the regulation of ADM formation in response to injury, this may be a Ras dependent or independent phenomenon. Examination of the role of *Etv5* in PanIN formation and carcinogenesis in the context of a constitutive oncogenic *Kras* mutation would be illuminating and is an area of active investigation.

It has been demonstrated that *Sox9* plays a critical role in the formation and maintenance of ADM which can be induced by ectopic expression of Sox9 (Kopp et al., 2012; Prevot et al., 2012; Chen et al., 2015). Of interest, we observed a spatial and temporal association of ETV5- and SOX9-expression in the context of acute pancreatitis. In the DBA lectin sorted ductal cell compartment of wild-type mice after cerulein induced pancreatitis, which contains cells that have undergone ADM, we found increased expression of both ETV5 and SOX9 at day 3. While ETV5 and SOX9 co-localize in ADMs in wild-type mice after induction of acute pancreatitis, the loss of *Etv5* is associated with loss of SOX9 expression in the limited number of ADMs that were observed in *Pdx1cre;Etv5*$^{fl/fl}$*;Rosa*^{YFP} mice.

Conversely, specific loss of *Sox9* did not alter the expression of ETV5 in pancreatitis and ADM, indicating a hierarchy in which *Etv5* seems to be located upstream of *Sox9*. Furthermore, expression of SOX9 was increased by almost seven-fold in ETV5-overexpressing pancreatic ductal cells forming hollow cystic structures in 3D organoid culture and ETV5 and SOX9 were noted to co-localize in these structures. Finally, the *Sox9* luciferase reporter construct confirmed ETV5- dependent regulation of the *Sox9* luciferase reporter gene. Overall, our data suggest an axis of ETV5 mediated regulation of SOX9, consistent with our previous work that PRRX1, a homeodomain transcriptional factor, may regulate Sox 9 directly as well (Reichert et al., 2013a). It is conceivable that tissue and context specific mechanisms may function for the converse to occur, namely that Sox9 may regulate Etv5, which we did not test. For example, Sox9 may regulate Etv5 in the regulation of male fertility (Alankarage et al., 2016), kidney development although biochemical evidence is lacking (Reginensi et al., 2011), and chondrosarcoma cells based upon functional transfection studies with indirect regulation by miR-145 (Mak et al., 2015). Elucidating these context-specific mechanisms in pancreatic ductal cells, pancreatitis, and PanIN remain an area of active interest and investigation.

Our data provide new mechanistic insight and define novel functional roles for *Etv5* in the regulation of ADM and pancreatic regeneration, through regulation of *SOX9*. This provides evidence for a possible new axis in the regulation of ductal morphogenesis with implications in our understanding of pancreatic homeostasis, pancreatitis and epithelial plasticity (Fig. 6).

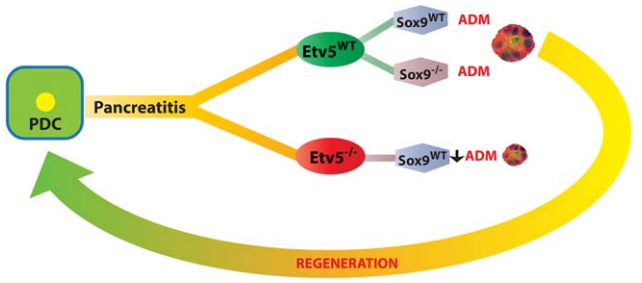

Fig. 6. Schematic of the suggested role of Etv5 in ADM formation and tissue regeneration.

Experimental Procedures

Pancreatic Ductal Cell Isolation

Primary PDC lines were isolated from *Pdx1Cre*; *Rosa26*^{YFP} (termed PDC) and *Etv5*$^{fl/fl}$*;Rosa*^{YFP} mice and cultured as described previously (Reichert et al., 2013b). Pancreata were dissected from mice, placed into a 50-ml beaker containing G solution on ice (1 L of HBSS (Gibco, Invitrogen, cat. no. 14175-04), 0.9 grams glucose and 47.6 μM $CaCl_2$), and minced into pieces $<1\,mm^3$ with sterile scissors. The supernatant is aspirated and the cells bathed in 10 ml of 4°C G solution twice before ~1 ml is transferred into a glass bottle containing a magnetic stir bar and 25 ml of 1 mg/ml collagenase type V (Sigma-Aldrich, cat. no. C9263) solution in DMEM/F12 (Gibco, Invitrogen, cat. no. 11330-032). This solution was incubated at 37°C in a water bath for 20 min with gentle stirring until atomized. The collagenase solution was quenched with chilled (4°C) G solution, and the mixture was centrifuged (300 g) for 5 min at 4°C. The pellet was resuspended with 1 ml of trypsin-ethylenediaminetetraacetic acid (EDTA; Gibco, Invitrogen, cat. no. 25300-054), incubated at room temperature for 5 min, and then resuspended with 2 ml of trypsin inhibitor (Sigma-Aldrich, cat. no. T6522). The solution was then diluted with 50 ml of G solution, centrifuged (300 g) for 5 min at 4°C, and the pellet resuspended in 10 ml of sorting buffer (PBS pH 7.2 containing 0.5% [wt/vol] bovine serum albumin [BSA] and 2 mM EDTA) at 4°C. The suspension was then filtered through a 40-μM cell strainer in a centrifuge (300 g) for 5 min at 4°C. The pellet was resuspended for downstream applications.

2D PDC Cell Culture

Cells were propagated on 2D culture using PDC full medium: 500 ml DMEM/F12, 5% Nu-Serum IV (BD Biosciences, cat. no. 355104), 1% penicillin-streptomycin (Gibco, Invitrogen, cat. no. 150140-122), bovine pituitary extract 25 μg/ml (BD Biosciences, cat. no. 354123), 2.5 ml ITS + Premix (BD Biosciences, cat. no. 354352), 20 ng/ml epidermal growth factor (BD Biosciences, cat. no. 354001), 100 ng/ml cholera toxin (Sigma-Aldrich, cat. no. C8052), 5 nM 3,3,5-triiodo-L-thyronine, 1 μM dexamethasone (Sigma-Aldrich, cat. no. D1756), 5 mg/ml glucose, and 1.22 mg/ml nicotinamide. Cell culture plates were coated with collagen mixture, 1.5 ml per well of a six-well plate (Costar, cat. no. 3516), and set for 45 min at 37°C: 100 μl of 10 × PBS, 0.0165 1N NaOH and ~1 ml of type I rat-tail collagen (final concentration of 2.31 mg/ml, varies per lot; BD Biosciences, cat. no. 354236). The PDC cell pellet was re-suspended in 1 ml of PDC full medium and divided on to culture plates with PDC full medium. Media was

TABLE 1. Primer Sequences

Application	Gene	5′ – 3′ FWD	5′ – 3′ REV
qPCR	mCyclo	ATGGTCAACCCCACCGTGT	TTCTGCTGTCTTTGGAACTTTGTC
	mEtv5	ACTTCCAGAACCTGGATCACAGCA	TGGCTTTCAGGCATCATCTTTGGC
	mK19	TCCCAGCTCAGCATGAAAGCT	AAAACCGCTGATCACGCTCTG
	mHnf1b	ACAATCCCAGCAATCTCAGAA	GCTGCTAGCCACACTGTTAATGA
	mSox9	CAAGACTCTGGGCAAGCTCTG	TCCGCTTGTCCGTTCTTCAC
	mPtf1a	TGCGCTTGGCCATAGGCTACATTA	AGATGATAACCTTCTGGGCCTGGT
	mMist1	AATAAGGAGGGTGAGTGGTTGGCA	AAGGAAGAGGCCAAGGACAAGTGA
	mFGF9	GAGAACTGGTACAACACCTACTC	CTTGGAGTCCCGTCCTTATTT
	mPGD2-Synthase	TCCTGGACACTACACCTACA	CTTGGTGCCTCTGCTGAATA
Cloning	mEtv5 (Age1, MluI)	TACAGACCGGTAGCACCATGGATGG GTTTTGTGATCAG	ATAGCACGCGTTTAGTAAGCGAA GCCTTCGGTGTAGGG
	Sox9-pGL3basic-luc (Mlu1,Xho1)	ACTGACGCGTACACACTTTCGTGG AGGCGTAGAA	ACTGCTCGAGAAATGTTTGGGT GACTCAACGCCC

changed every other day. Passage was completed at 80% confluence by transferring the collagen sheet into a 50-ml conical tube with 9 ml of 1 mg/ml type V collagenase (Sigma-Aldrich, cat. no. C9263) for 20 min at 37°C. The suspension was pelleted (300 g for 5 min at 4°C), incubated with trypsin-EDTA 0.035% (5 min at room temperature), and then incubated with soybean trypsin inhibitor and 25 ml of cold G solution. The pellet was resuspended in PDC full media onto collagen-coated plates.

3D Organoid PDC Culture

The 3D cultures were performed by first preparing collagen solution: L-glutamine (1:8.5), $NaHCO_3$ 7.5% solution (1:32.5), MEM 10 × (Invitrogen, cat. no. 11430030) (1:10.2), Nutragen bovine collagen I (Advanced BioMatrix, cat. no. 5010-D) (1:3.1), HEPES (Sigma-Aldrich, cat. no. H0887) (1:51), Sterile H_2O (1:2.5). Each well of four-well chamber slide (Nunc 177437; Thermo Fisher Scientific, cat. no. 12-565-21) was coated with 225 μl of collagen solution and set at 37°C for 45 min. The concentration of the PDC cell suspension was adjusted to $0.5–2.0 \times 10^5$ cells/ml in PDC full medium with attention to create a single cell suspension. A total of 50 μl of PDC solution (in PDC full medium) was added to 350 μl of liquid collagen solution, mixed, and pipetted on top of the solidified bottom collagen layer in the chamber slide which was again set at 37°C for 45 min.

Subsequently, 500 μl of PDC full media was added to the chamber slide and changed every other day. Cells were cultured in a 37°C incubator with 5% CO_2. To harvest cells from 3D culture, the collagen block was placed into a 50-ml conical tube with 5 mg collagenase (Sigma cat. no. C9263) in 5 ml DMEM/F12 and incubated at 37°C for 20 min. The mixture was brought to 50 ml with DMEM/F12 and pelleted (300 g, 5 min), trypsinized with trypsin-EDTA (5 min at room temperature), and incubated with soy bean trypsin inhibitor (5 min at room temperature). The resultant pellet was used for downstream applications.

For cyst quantification, 5×10^3 cells were seeded per chamber of a four-well chamber slide incubated in a humidified incubator at 37°C and 5% CO_2. The number of cysts was assayed 48 hr after seeding by counting 10 high power fields per well of a four-well chamber. Assays were performed independently three times.

Mouse Ductal Cell Labeling and Cell Separation

To enrich extracted cell populations for ductal cell extracts, DBA lectin sorting was completed. Cells were isolated from a mouse pancreata as described above and suspended with 1:200 diluted DBA lectin–fluorescein isothiocyanate (FITC; Vector Labs, cat. no. FL-1031) and incubated for 10 min in the dark at 4°C on a rotor. Cells were washed with 700 μl of separation buffer (PBS, 0.5% BSA, and 2 mM EDTA) and centrifuged for 10 min at 300g at 4°C. The pellet was resuspended in 90 μl of separation buffer and 10 μl of anti-FITC MicroBeads (Miltenyi Biotec, cat. no. 130-048-701) and incubated on a rotor at 4°C for 15 min. The cells were washed with 1 ml of sorting buffer (PBS, 0.5% BSA, 2 mM EDTA) and the pellet (300 g for 10 min) was resuspended in 500 μl of sorting buffer. MACS Separation (MS) columns (Miltenyi Biotec, cat. no. 130-042-201) were prepared by running 500 μl of chilled sorting buffer and then the labeled cell suspensions (500 μl) were applied to the column. The columns were washed three times with 500 μl of buffer and the flow through was collected as the DBA lectin–negative fraction. The column was removed from the magnetic field and 1,000 μl of separation buffer was then added with a plunger to collect the DBA lectin–positive fraction. The samples were spun down (300 g for 15 min at 4°C), and the pellets were used for downstream applications.

Lentiviral Transduction and Vector Constructs

Etv5 was amplified from genomic cDNA (Table 1). Following PCR amplification, coding sequences were digested using Age1 and Mlu1 and subcloned into pTRIPZ (RHS4743; Open Biosystems). LV-Cre was obtained from Addgene (Plasmid #12106). PDCs were grown as described above, seeded at 1×10^5 cells per well onto a collagen-coated six-well plate (one plate for each virus), and grown for 24 hr in PDC full media. Each well was then replaced with 2 ml of PDC full medium containing 4 μg/ml polybrene (EMD Millipore, cat. no. TR-1003-G) and 400 μl of virus. The plate was then centrifuged (550 g for 1 hr at 32°C), aspirated, and then centrifuged again with a fresh mixture of media, polybrene and virus. Parental cell lines were transduced in parallel with Etv5/LV-Cre constructs or empty vector constructs (Control). Subsequently, cells were grown in PDC full media and drug selection with puromycin (Sigma-Aldrich, cat. no. P8833) (5 μg/ml)

was performed. In the case of LV-cre on PDCs from mice that harbor a *Rosa26^{YFP}* allele, FACS was then used to enrich for a YFP-positive fraction of cells.

Luciferase Reporter Assay

Luciferase reporter assays were performed using a Luciferase Assay Kit (Promega). In brief, PDC control or PDC mEtv5 cells were plated onto 12-well plates at a density of 1×10^5 cells per well. A total of 500 ng of pGL3-basic (Promega) or pGL3-Sox9-Promoter (-2484 bp to -584 bp) (Table 1) were transfected into PDC control or PDC mEtv5 cells with Lipofectamine 2000 (Life Technologies, Grand Island, NY). Forty-eight hours after transfection, cells were lysed in 150 ml of passive lysis buffer and assayed for luciferase activity using the Pierce Firefly Luciferase Glow assay kit (Thermo Scientific, Rockford, IL). Three independent experiments were performed.

Quantitative Real-Time-qPCR

RNA was isolated using RNeasy Mini Kit (QIAGEN) from cells grown in 3D or 2D culture as described above. One microgram of RNA was transcribed into cDNA (Taqman Reverse Transcription Reagents) and assayed using quantitative real-time (RT) PCR with Power SYBR Master Mix (Applied Biosystems) on the StepOnePlus System (Applied Biosystems). Primers are listed in Table 1. $P < 0.05$ was statistically significant (two-sided Mann-Whitney Wilcoxon test). Error bars represent the standard deviation. Three independent experiments were performed.

Western Blotting

PDCs were grown in 2D culture to 80% confluence and harvested as described above. Cell pellets were lysed in RIPA buffer plus protease and phosphatase inhibitor cocktail (Thermo Fisher Scientific). Protein concentration was normalized using Bradford reagent (Bio-Rad, Hercules, CA). For every sample, 20 μg was resolved on 4–12% Bis-Tris gels (Invitrogen, Carlsbad, CA), and transferred to polyvinylidene difluoride membranes. Membranes were blocked in either PBS containing 0.05% Tween and 5% nonfat dry milk or in blocking buffer (LiCor, Lincoln, NE) for 1 hr at room temperature and incubated with one of the following antibodies at 4°C overnight: Anti-Etv5 Antibody (1:100; Abcam ab102010) and anti-mouse β-actin (1:5,000, A5316, Sigma-Aldrich). Visualization was performed with the appropriate horseradish peroxidase-coupled secondary antibody (GE Healthcare, Piscataway, NJ) and Western Lightning ECL reagents (Perking Elmer, Waltham, MA) on Hyperfilm ECL (GE Healthcare).

Generation and Analysis of Conditional Etv5 Knockout

The Institutional Animal Care and Use Committee of the University of Pennsylvania approved all animal studies (Protocol #8050-30). A previously generated conditional knockout of *Etv5* (Zhang et al., 2009), was bred into the *Rosa26^{YFP};Cre* background. The *Etv5$^{fl/fl}$* mice were a generous gift from Dr. Xin Sun (University of Wisconsin, Madison, WI). The *Pdx1Cre* was derived from Melton and colleagues (Gu et al., 2002) and recombination was verified by robust expression of YFP on sacrifice.

Cerulein Induced Pancreatitis

Acute pancreatitis was induced as described previously (Siveke et al., 2008; Lerch and Gorelick, 2013). In brief, after a fasting period of 18 hr, 8- to 12-week-old *Pdx1-cre; Rosa26^{YFP}*, *Pdx1-cre;Etv5$^{fl/WT}$;Rosa26^{YFP}*, or *Pdx1-cre;Etv5$^{fl/fl}$;Rosa26^{YFP}* mice were injected intraperitoneally with cerulein (C9026, Sigma-Aldrich). Mice were injected over 2 consecutive days with eight hourly injections per day. A total of 200 microliters of 10 mg/ml cerulein (50 mg/kg body weight) was administered per injection. Control animals received 0.9% saline. Cohorts of three mice per genotype, per time point were performed for saline injected, day 1, day 3, day 7, and day 21 after injection. A similar protocol of cerulein induced pancreatitis was performed on *Ptf1a^{CreER};Sox9$^{fl/fl}$Rosa26^{YFP}* mice, except these were analyzed on day 2 and day 7 after injection (Kopp et al., 2011, 2012).

Histologic severity of pancreatitis was assessed per a previously validated rubric (Rongione et al., 1997), graded by two independent reviewers blinded to the treatment or genotype using serial hematoxylin and eosin (H&E) sections. ADM were quantified histologically by two independent reviewers blinded to the treatment or genotype histologically and confirmed by serial sections stained for K19 and amylase as detailed below. A total of 7 random, representative fields from each pancreata were examined for histologic and ADM quantifications. All Graphs are displayed with 21 fields examined and standard error of the mean.

Immunohistochemical/IF Staining and Image Analysis

Immunohistochemisty (IHC) and IF staining were carried out as described previously (Burstin et al., 2010; Heeg et al., 2016). Tissue was fixed in zinc formalin overnight, transferred to 70% ethanol and submitted to the University of Pennsylvania Molecular Pathology and Imaging Core where paraffin-embedded sections were cut for H&E staining and IHC/IF.

After warming at 60°C, slides were deparaffinized with a series of xylene and graded ethanol washes and antigen retrieval was performed with 10 mM citric acid buffer (pH 6.0) in a pressure cooker for 1 hr. Sections were washed with PBS and blocked using TBS + 0.3% Triton X-100 (TBS-T) with 5% normal donkey serum (Jackson ImmunoResearch) for 1 hr at room temperature. Primary antibodies were incubated at the appropriate dilutions in 5% donkey serum, TBS-T overnight at 4°C: anti-Etv5 (1:200; Abcam ab102010), anti-green fluorescent protein (1:250; Abcam ab13970), anti-Amylase (1:200, Santa Cruz C20), anti-K19 (1:50, TROMAIII, Developmental Studies Hybridoma Bank), and anti-Sox9 (1:100; Santa Cruz SC-17340). After two washes with TBS-Tween, secondary antibodies (cy2- and/or cy3- and/or cy5-conjugated secondary immunoglobulin G antibodies at 1:600 dilution) were applied and incubated for 30 min at 37°C. DAPI (1:1,000) counterstaining was performed (Sigma-Aldrich). Slides were mounted in Vectashield mounting medium (Vector Laboratories, Burlingame, CA). Images were acquired using a Nikon E600 microscope using Plan Fluor Objectives: 4× (NA 0.13), 10× (NA 0.30), 20× (NA 0.5). Imaging was performed with a QICAM (Q Imaging #32-0090B-531) camera at 1 × 1 binning. Image acquisition was performed using iVision 4.0.14 software.

For PDCs imaged in 3D organoid culture (Fig. 4B), collagen cultures were treated with 1 mg/ml collagenase solution (Sigma-Aldrich, cat. no. 27991 mg/ml) at 37°C for 10 min, washed with PBS, and then fixed in 4% paraformaldehyde (PFA) for 30 min at

room temperature. After washing with PBS, they were incubated for 30 min at room temperature in a 0.025% saponin, fish skin gelatin permeabilization solution (Sigma-Aldrich, cat. no. G7765) in PBS and 0.005% Triton X-100. Primary and secondary antibodies were diluted in permeabilization solution and incubations were overnight at 4°C: anti-Etv5 (1:200; Abcam ab102010), anti-Sox9 (1:100; Santa Cruz SC-17340), Cy2-donkey anti-rabbit 1:400 (Molecular Probes, Eugene, OR), and Cy3- donkey anti-goat 1:400 (Molecular Probes, Eugene, OR). After antibody incubations, cultures were postfixed in 4% PFA, counterstained with DAPI, and mounted directly onto slides with ProLong mounting media (Invitrogen, Carlsbad, CA). Fixed and stained cysts were photographed on a Nikon Eclipse Ti-U microscope using Plan Fluor Objectives, 4 × (NA 0.13) and 10 × (NA 0.30). Images were taken with Hamamatsu ORCA-ER #C4742-95-12ERG with 1 × 1 binning on iVision 4.0.14 software.

TUNEL assays were performed using the in situ cell death detection kit (Roche, Mannheim, Germany). TUNEL assay were graded as positive cells per high power field with 10 high power fields examined in three animals per group. $P < 0.05$ was statistically significant (two-sided Mann-Whitney Test).

Semiquantitative grading of amylase area was performed using semi-automated ImageJ software analysis with the same threshold for each animal; results were expressed as percentage staining per visual field per DAPI positive area. A minimum of three animals per genotype, per day and seven different high power fields per animal were examined for quantification.

Statistical Analysis

For all experiments, statistical analyses were performed using the nonparametric, two-sided Mann-Whitney test, except where noted otherwise. $P < 0.05$ was considered statistically significant. Number of mice (n) is indicated in each experiment. The number of biological and technical replicates is specified in the figure legend or in the Material and Methods Section, respectively. Values are expressed as mean ± SEM.

Acknowledgments

The authors have no disclosures. S.T., M.R., and A.K.R. were funded by the NIH, K.D., J.K.L. and M.S. were funded by NIH/NIDDK, M.R. was funded by the National Pancreas Foundation, S.H. was funded by the Deutsche Krebshilfe, M.R. and A.N. were funded by the Max Eder Program, M.R. received an AGA-Actavis Research Award in Pancreatic Disorders, S.T. was funded by the Honjo International Scholarship, J.L.K. received a JDRF Advanced Postdoctoral Fellowship, and A.K.R. was funded by the NIH/NIDDK P30-DK050306 Center for Molecular Studies in Digestive and Liver Diseases (Molecular Pathology and Imaging, Molecular Biology/Gene Expression, Cell Culture, and Transgenic and Chimeric Mouse Cores), and American Cancer Society Grant RP-10-033-01-CCE.

References

Alankarage D, Lavery R, Svingen T, Kelly S, Ludbrook L, Bagheri-Fam S, Koopman P, Harley V. 2016. SOX9 regulates expression of the male fertility gene Ets variant factor 5 (ETV5) during mammalian sex development. Int J Biochem Cell Biol 79:41–51.

Ardito CM, Grüner BM, Takeuchi KK, Lubeseder-Martellato C, Teichmann N, Mazur PK, DelGiorno KE, Carpenter ES, Halbrook CJ, Hall JC, Pal D, Briel T, Herner A, Trajkovic-Arsic M, Sipos B, Liou G-Y, Storz P, Murray NR, Threadgill DW, Sibilia M, Washington MK, Wilson CL, Schmid RM, Raines EW, Crawford HC, Siveke JT. 2012. EGF receptor is required for KRAS-induced pancreatic tumorigenesis. Cancer Cell 22:304–317.

Burstin von J, Reichert M, Wescott MP, Rustgi AK. 2010. The pancreatic and duodenal homeobox protein PDX-1 regulates the ductal specific keratin 19 through the degradation of MEIS1 and DNA binding. PLoS One 5:e12311.

Chen N-M, Singh G, Koenig A, Liou G-Y, Storz P, Zhang J-S, Regul L, Nagarajan S, Kühnemuth B, Johnsen SA, Hebrok M, Siveke J, Billadeau DD, Ellenrieder V, Hessmann E. 2015. NFATc1 Links EGFR signaling to induction of Sox9 transcription and acinar-ductal transdifferentiation in the pancreas. Gastroenterology 148: 1024–1034.e9.

Chotteau-Lelievre A, Montesano R, Soriano J, Soulie P, Desbiens X, de Launoit Y. 2003. PEA3 transcription factors are expressed in tissues undergoing branching morphogenesis and promote formation of duct-like structures by mammary epithelial cells in vitro. Dev Biol 259:241–257.

Collins MA, Yan W, Sebolt-Leopold JS, Pasca di Magliano M. 2014. MAPK signaling is required for dedifferentiation of acinar cells and development of pancreatic intraepithelial neoplasia in mice. Gastroenterology 146:822–834.e7.

Giroux V, Rustgi AK. 2017. Metaplasia: tissue injury adaptation and a precursor to the dysplasia-cancer sequence. Nat Rev Cancer 17:594–604.

Gruber R, Panayiotou R, Nye E, Spencer-Dene B, Stamp G, Behrens A. 2016. YAP1 and TAZ control pancreatic cancer initiation in mice by direct up-regulation of JAK-STAT3 signaling. Gastroenterology 1:526–539.

Gu G, Dubauskaite J, Melton DA. 2002. Direct evidence for the pancreatic lineage: NGN3 + cells are islet progenitors and are distinct from duct progenitors. Development 129:2447–2457.

Haumaitre C, Barbacci E, Jenny M, Ott MO, Gradwohl G, Cereghini S. 2005. Lack of TCF2/vHNF1 in mice leads to pancreas agenesis. Proc Natl Acad Sci U S A 102:1490–1495.

Heeg S, Das KK, Reichert M, Bakir B, Takano S, Caspers J, Aiello NM, Wu K, Neesse A, Maitra A, Iacobuzio-Donahue CA, Hicks P, Rustgi AK. 2016. ETS-Transcription Factor ETV1 regulates stromal expansion and metastasis in pancreatic cancer. Gastroenterology 151:540–553.e14.

Jacquemin P, Durviaux SM, Jensen J, Godfraind C, Gradwohl G, Guillemot F, Madsen OD, Carmeliet P, Dewerchin M, Collen D, Rousseau GG, Lemaigre FP. 2000. Transcription factor hepatocyte nuclear factor 6 regulates pancreatic endocrine cell differentiation and controls expression of the proendocrine gene ngn3. Mol Cell Biol 20:4445–4454.

Jacquemin P, Lemaigre FP, Rousseau GG. 2003. The Onecut transcription factor HNF-6 (OC-1) is required for timely specification of the pancreas and acts upstream of Pdx-1 in the specification cascade. Dev Biol 258:105–116.

Ji B, Tsou L, Wang H, Gaiser S, Chang DZ, Daniluk J, Bi Y, Grote T, Longnecker DS, Logsdon CD. 2009. Ras activity levels control the development of pancreatic diseases. Gastroenterology 137: 1072–1082.e6.

Kar A, Gutierrez-Hartmann A. 2013. Molecular mechanisms of ETS transcription factor-mediated tumorigenesis. Crit Rev Biochem Mol Biol 48:522–543.

Kobberup S, Nyeng P, Juhl K, Hutton J, Jensen J. 2007. ETS-family genes in pancreatic development. Dev Dyn 236:3100–3110.

Kopp JL, Dubois CL, Schaffer AE, Hao E, Shih HP, Seymour PA, Ma J, Sander M. 2011. Sox9 + ductal cells are multipotent progenitors throughout development but do not produce new endocrine cells in the normal or injured adult pancreas. Development 138:653–665.

Kopp JL, von Figura G, Mayes E, Liu F-F, Dubois CL, Morris JP IV, Pan FC, Akiyama H, Wright CVE, Jensen K, Hebrok M, Sander M. 2012. Identification of Sox9-dependent acinar-to-ductal reprogramming as the principal mechanism for initiation of pancreatic ductal adenocarcinoma. Cancer Cell 22:737–750.

Krah NM, De La O JP, Swift GH, Hoang CQ, Willet SG, Chen Pan F, Cash GM, Bronner MP, Wright CV, MacDonald RJ, Murtaugh LC. 2015. The acinar differentiation determinant PTF1A inhibits initiation of pancreatic ductal adenocarcinoma. eLife 4:9169.

Lerch MM, Gorelick FS. 2013. Models of acute and chronic pancreatitis. Gastroenterology 144:1180–1193.
Mak IWY, Singh S, Turcotte R, Ghert M. 2015. The epigenetic regulation of SOX9 by miR-145 in human chondrosarcoma. J Cell Biochem 116:37–44.
Miyamoto Y, Maitra A, Ghosh B, Zechner U, Argani P, Iacobuzio-Donahue CA, Sriuranpong V, Iso T, Meszoely IM, Wolfe MS, Hruban RH, Ball DW, Schmid RM, Leach SD. 2003. Notch mediates TGFα-induced changes in epithelial differentiation during pancreatic tumorigenesis. Cancer Cell 3:565–576.
Oh S, Shin S, Janknecht R. 2012. ETV1, 4 and 5: an oncogenic subfamily of ETS transcription factors. Biochim Biophys Acta 1826:1–12.
Payne SN, Maher ME, Tran NH, Van De Hey DR, Foley TM, Yueh AE, Leystra AA, Pasch CA, Jeffrey JJ, Clipson L, Matkowskyj KA, Deming DA. 2015. PIK3CA mutations can initiate pancreatic tumorigenesis and are targetable with PI3K inhibitors. Oncogenesis 4:e169.
Pierreux CE, Poll AV, Kemp CR, Clotman F, Maestro MA, Cordi S, Ferrer J, Leyns L, Rousseau GG, Lemaigre FP. 2006. The transcription factor hepatocyte nuclear factor-6 controls the development of pancreatic ducts in the mouse. Gastroenterology 130:532–541.
Pin CL, Rukstalis JM, Johnson C, Konieczny SF. 2001. The bHLH transcription factor Mist1 is required to maintain exocrine pancreas cell organization and acinar cell identity. J Cell Biol 155: 519–530.
Pin CL, Ryan JF, Mehmood R. 2015. Acinar cell reprogramming: a clinically important target in pancreatic disease. Epigenomics 7: 267–281.
Prevot PP, Simion A, Grimont A, Colletti M, Khalaileh A, Van den Steen G, Sempoux C, Xu X, Roelants V, Hald J, Bertrand L, Heimberg H, Konieczny SF, Dor Y, Lemaigre FP, Jacquemin P. 2012. Role of the ductal transcription factors HNF6 and Sox9 in pancreatic acinar-to-ductal metaplasia. Gut 61:1723–1732.
Puri S, Folias AE, Hebrok M. 2015. Plasticity and dedifferentiation within the pancreas: development, homeostasis, and disease. Cell Stem Cell 16:18–31.
Reginensi A, Clarkson M, Neirijnck Y, Lu B, Ohyama T, Groves AK, Sock E, Wegner M, Costantini F, Chaboissier M-C, Schedl A. 2011. SOX9 controls epithelial branching by activating RET effector genes during kidney development. Hum Mol Genet 20:1143–1153.
Reichert M, Takano S, Burstin von J, Kim SB, Lee JS, Ihida-Stansbury K, Hahn C, Heeg S, Schneider G, Rhim AD, Stanger BZ, Rustgi AK. 2013a. The Prrx1 homeodomain transcription factor plays a central role in pancreatic regeneration and carcinogenesis. Genes Dev 27:288–300.
Reichert M, Rustgi AK. 2011. Pancreatic ductal cells in development, regeneration, and neoplasia. J Clin Invest 121:4572–4578.
Reichert M, Takano S, Heeg S, Bakir B, Botta GP, Rustgi AK. 2013b. Isolation, culture and genetic manipulation of mouse pancreatic ductal cells. Nat Protoc 8:1354–1365.
Rongione AJ, Kusske AM, Kwan K, Ashley SW, Reber HA, McFadden DW. 1997. Interleukin 10 reduces the severity of acute pancreatitis in rats. Gastroenterology 112:960–967.
Seymour PA, Freude KK, Tran MN, Mayes EE, Jensen J, Kist R, Scherer G, Sander M. 2007. SOX9 is required for maintenance of the pancreatic progenitor cell pool. Proc Natl Acad Sci U S A 104:1865–1870.
Shi G, DiRenzo D, Qu C, Barney D, Miley D, Konieczny SF. 2012. Maintenance of acinar cell organization is critical to preventing Kras-induced acinar-ductal metaplasia. Oncogene 32:1950–1958.
Siveke JT, Lubeseder-Martellato C, Lee M, Mazur PK, Nakhai H, Radtke F, Schmid RM. 2008. Notch signaling is required for exocrine regeneration after acute pancreatitis. Gastroenterology 134: 544–555.
Srinivas S, Watanabe T, Lin C-S, William CM, Tanabe Y, Jessell TM, Costantini F. 2001. Cre reporter strains produced by targeted insertion of EYFP and ECFP into the ROSA26 locus. BMC Dev Biol 1:4.
Thayer SP, di Magliano MP, Heiser PW, Nielsen CM, Roberts DJ, Lauwers GY, Qi YP, Gysin S, Fernández Del Castillo C, Yajnik V, Antoniu B, McMahon M, Warshaw AL, Hebrok M. 2003. Hedgehog is an early and late mediator of pancreatic cancer tumorigenesis. Nature 425:851–856.
Yuen H-F, Chan Y-K, Grills C, McCrudden CM, Gunasekharan V, Shi Z, Wong AS-Y, Lappin TR, Chan K-W, Fennell DA, Khoo U-S, Johnston PG, El-Tanani M. 2011. Polyomavirus enhancer activator 3 protein promotes breast cancer metastatic progression through Snail-induced epithelial-mesenchymal transition. J Pathol 224:78–89.
Zhang Z, Verheyden JM, Hassell JA, Sun X. 2009. FGF-regulated Etv genes are essential for repressing Shh expression in mouse limb buds. Dev Cell 16:607–613.